JUNE 1989

MEETING NOTICE

The next meeting will be **June 16th**, at *CRAGIN FEDERAL SAVINGS & LOAN* 333 W. Wesley St. Wheaton, Ill. -Time - 7:30 P.M. *sharp.* Guests are welcome and need not be members to attend the meeting.

THE PRES SAYS

Four members had cars in the LaGrange Pet Parade on June 3rd ; Henry Setton, Ray Oviyach, Bill Shafer and George Krajnovich. Rain dampened, but did not cancel the event.

There have been several suggestions about our cars in July 4th parades. In my opinion, we can be better-represented if three cars can be in each parade. We will briefly discuss this topic on June 16.

John Newton's calculations of hybrid vehicle performance with the Newton motor, rated 200 amps - 100 volts, is included with this bulletin issue. The resulting performance is ok, but probably not exactly what we want. I propose at the next meeting to reach a final conclusion concerning performance aand ask a study group to take over and develop a final hybrid design proposal.

Bill

F. V. E. A. A.

FOX VALLEY ELECTRIC
AUTO ASSOCIATION
624 Pershing St. Wheaton, Il 60187

FIRST CLASS

ADDRESS CORRECTION
REQUESTED

MINUTES OF MAY 19, 1988 FVEAA MEETING

There were 14 members present at the meeting.

Treasurer Vana reported account balances of $ 848.28 in the savings account and $ 1189.97 in the checking account.

Member Vana reported on arrangements for the La Grange Pet Parade participation on June 3d. Tentatively, 6 FVEAA cars are expected; Setton, Johnson, Oviyach, Shafer, Stockberger, and Krajnovich.

President Shafer reported on arrangements for completion of the Club Car donation to Triton at their Board Meeting on May 23.

Member Stockberger noted the Fox Valley Hamfest at Pheasant Run on July 16th. No FVEAA car exhibition was discussed.

There was a brief continuation of the hybrid design project. Member Newton's calculations will be included with the next issue of the Newssletter.

Bill Shafer

William H. Shafer
(Secretary Pro-tem
In Paul Harris absence)

New DieHard battery built in Geneva

Sears and Johnson Controls recently introduced the Sears DieHard Gold.

The DieHard Gold, now the top-of-the-line battery for Sears, will be available in Sears automotive centers nationwide.

Johnson Controls designed, engineered and now manufactures the DieHard Gold at nine of its 12 battery assembly plants including the facility in Geneva.

This second generation DieHard is the most powerful battery in its class.

It outdistances all other national brands in the group 24 size with its combination of 900 cold cranking amps and 135 minutes of reserve capacity.

A feature exclusive to the DieHard Gold is an electro-flo system (patent pending) that was developed by Johnson Controls engineers. A plastic pump located along the interior wall of each battery cell prevents acid/electrolyte stratification.

The electro-flo system continuously mixes acid during the vehicle's normal stop-and-go driving. The pump mixes the sulfuric acid and water, then helps circulate the electrolyte evenly across the plates which hold the active materials.

Since the DieHard name was introduced in 1967, 67 million units have been sold.

The partnership between Sears and Johnson Controls dates back to the 1920s when Johnson Controls first built manufacturing plants to supply Sears with batteries.

ST. CHARLES CHRONICLE, BATAVIA CHRONICLE, GENEVA CHRONICLE, ELBURN CHRONICLE

Friday, May 12, 1989 BUSINESS/PEOPLE Page 9

FOX VALLEY PETRO-ELECTRIC VEHICLE
With the Newton Motor

Motor Characteristics

Voltage - 100 Volts
Current - 200 Amps
Power - 20 Horsepower
Speed - 3000/6000 RPM

$$\text{Torque} = \frac{(5250)\ (20)}{3000} = 35 \text{ Ft-lb}$$

Use 42

Design Assumptions

Curb Weight - 2700 Lbs
Wheel/Tire Radius - 1 foot
Final drive ratio - 4:1

Gear Ratio - 1st = 4:1
2nd = 2.5:1
3d = 1.3:1
4th = 1.0:1

Acceleration Calculation

Elapsed Time (Sec)	Ft/Min	MPH	RPM Wheel	RPM Motor	Volts	Amps	Kw
1	480	5.45	76	1216	41	250	10.2
2	960	10.90	152	2432	83	250	20.7
3	1440	16.35	228	3648	100	250	25.0
4	Shift requires 1 second						
5	1740	19.75	276	2760	40	250	22.5
6	2040	23.15	323	2760	100	250	25.0
7	2340	26.55	370	3700	100	250	25.0
8	2640	30.00	417	4170	100	250	25.0
9	Shift requires 1 second						
10	2796	31.8	445	2314	79	250	25.0
11	2952	33.5	470	2444	82	250	25.0

John S Newton
5/11/89

Solar-power car races way into fans' hearts

By Dan Jedlicka
Auto Writer

Looking like an extraterrestrial sports car, the solar-powered Sunraycer zoomed around the Museum of Science and Industry's parking lot last week in front of wide-eyed museum visitors.

No higher than a young child at three feet, the $2 million, one-seat Sunraycer was designed by 16 General Motors Corp.'s organizations and AeroVironment Inc.

It made almost no sound and appeared to glide over the concrete in front of the museum, where it will be exhibited through May 29.

"Most know of the Sunraycer because it got international acclaim after winning the first transcontinental World Solar Challenge race in Australia in November, 1987," said Bob Francis, a member of the Sunraycer project.

The car's average speed during the 1,950-mile race was 41.6 m.p.h. Francis said the race was no easy affair, "with dead kangaroos blocking roads and enormous, moisture-loving bush flies making life miserable if one dared stand in one spot for a minute."

The Sunraycer's power is derived from an 87-square-foot solar array, which uses solar cells usually designed to power communciations satellites. Surplus energy is stored in advanced-design batteries.

The super-long, super-wide Sunraycer's powerful motor weighs only 11 pounds and produces 2 horsepower, up to 40 percent more than commercially available motors of similar size. It can generate up to 10 horsepower for brief periods.

"The Sunraycer no longer will race but will influence design of GM electric vehicles," said George Ettenheim, who was driving the vehicle at the museum and is another member of the Sunraycer project.

The 390-pound Sunraycer has a teardrop-shaped body made of light composite materials and bicycle tires with aluminum-rimmed wheels for the least possible rolling resistance. It has virtually no wind drag.

The vehicle represents development and demonstration of advanced technology as applied to aerodynamic design, lightweight structures and materials, electric motors, suspension, steering systems, high-efficiency batteries, solar arrays and power electronics.

"All that may lead to important practical applications in other types of vehicles," GM said.

Vehicles influenced by the Sunraycer may be closer than some think because of the push in California for lower car emissions and strong sentiment in Congress concerning better auto fuel economy, industry observers note.

Ettenheim, who has traveled extensively with the Sunraycer tour, said, "Young motorists with fast cars are amazed it can hit 83 m.p.h. Elderly people love it because they figure they would never live to see anything like it.

"Everyone seems to like the fact it generates absolutely no pollution."

SUN-TIMES / Al Podgorski

The solar-powered Sunraycer zooms around the Museum of Science and Industry's parking lot in front of wide-eyed museum visitors. Molly McCardle of the Sunraycer team checks out driver George Ettenheim (above), while Doug Peters of the racing team keeps an eye on the course (left).

FRANK & ERNEST

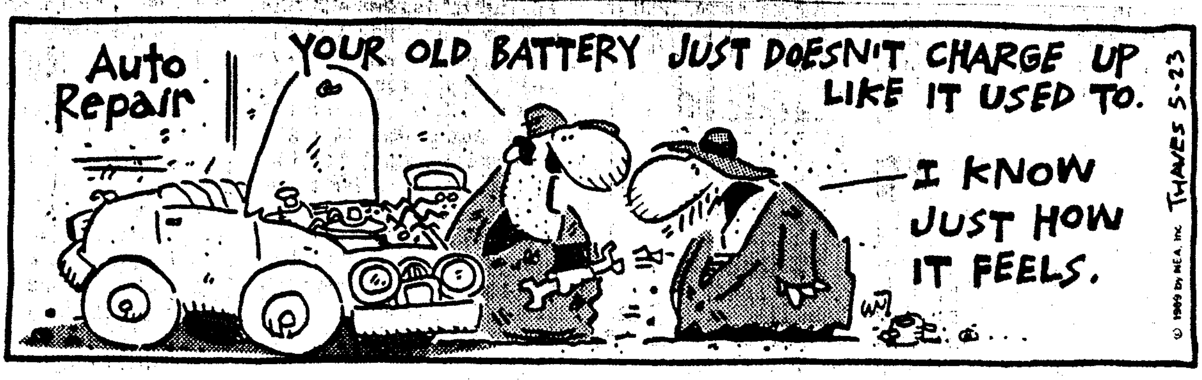

Liquid-Cooled Inverter Drives Electric Vehicle's 70 HP Motor

R.D. King, F.G. Turnbull, E. Delgado and P.M. Szczesny/GE Corporate R&D

A PWM inverter using a liquid-cooled, three-phase Darlington power module furnishes the drive for an interior permanent magnet, 70 HP motor in an electric vehicle drive system.

Specifically designed for an electric vehicle, a three-phase transistor inverter employs a 204V battery supply and drives an interior permanent magnet (IPM) synchronous motor. A microprocessor-based controller works with the inverter to regulate drive operation using motor phase current and rotor position feedback. *Figure 1* is a simplified block diagram of the system and *Table 1* lists the inverter's electrical requirements.

The inverter converts the battery voltage into an adjustable AC current and frequency with either a positive or negative phase sequence for the IPM motor. The direction of power flow is also reversible: from DC to AC during motoring and from AC to DC during regeneration. Vehicle requirements and system constraints determined power magnitude, maximum frequency, extent of pulse width modulation, and maximum and minimum DC voltage levels. The program's goal was to improve the total system efficiency relative to the Federal Urban Driving Schedule (FUDS).

The 96% efficient IPM motor operates from a 135V battery (101.4V line-to-line). It produces 81 lb-ft in the constant torque region and 70 HP from its base speed of about 4500 RPM to 11,000 RPM. *Figure 2* shows the motor's maximum torque envelope for an inverter with peak current capability of 200A, 400A, and this electric transaxle, ETX-II, power module's 525A. Projected output horsepower levels are shown in the constant power regions for the 400 and 525A modules. Motor stack length is 7.5 in. and the stator is 8.75 in. in diameter. Combined rotor and stator weight is 112 lbs., consisting of 90.9 lbs. of steel, 16.9 lbs. of copper and 4.2 lbs. of Nd-Fe-B magnets.

The inverter power circuit (*Figure 3*) is a three-phase, full-wave bridge with six GE ZJ704E power Darlington transistors and a reverse-connected feedback diode. Each transistor has a base drive circuit (BD) and polarized snubber (S) for load line shaping during switching.

Ratings of the power Darlington transistors are 200A collector current, 550V V_{CEX}, collector-emitter saturation voltage of 1.2 to 1.6V at 200A, and a gain of 100 at 200A collector current. A peak current requirement of 525A requires three paralleled Darlington chips. The single reverse-connected diode is rated for the full current.

Power Module

A schematic of a phase-leg power module is shown in *Figure 4*. The polarized snubber consists of a fast diode (EJ5), 5Ω resistor, and 0.68μF capacitor. A smaller RC network, 1Ω and 0.047μF, reduces the very high frequency components of the snubber diode's voltage. An external "speed-up" diode (GE1102) connects the Darlington's bases.

Base drive for the Darlingtons is 6.5A during the transistor conduction interval. During turn-off, a −6.5A pulse removes current from the base. A −2V applied to the base-emitter junction during the off-time prevents the Darlington from carrying

Table 1. Inverter Electrical Requirements

Nominal battery voltage	204-VDC
Max. motor horsepower	70-HP
Max. motor frequency (to meet ratings)	366.7-Hz
Max. motor frequency (overspeed)	450-Hz
Max. motoring current in PWM	315-A RMS
Max. motoring current in square-wave	325-A RMS
Min. battery voltage (to meet ratings)	125-VDC
Max. battery voltage during regnerating	265-VDC
Max. regenerating current in PWM	125-A RMS
Peak transistor or diode current at 204V	525A
Max. switching frequency in PWM	4000-Hz

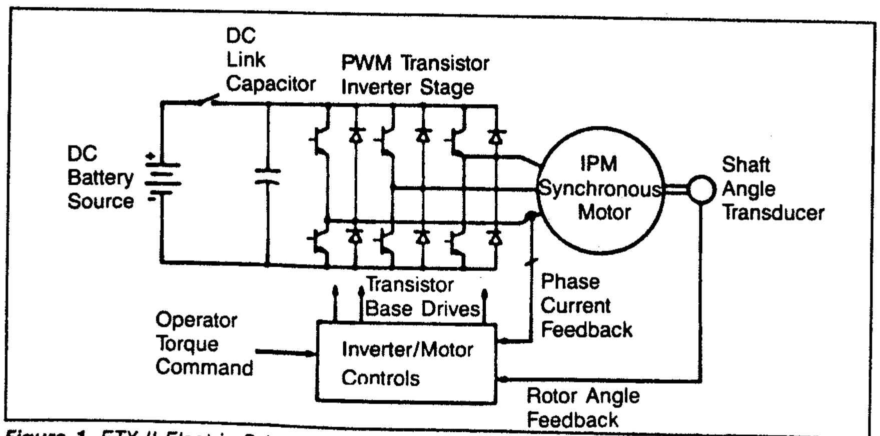

Figure 1. ETX-II Electric Drive System.

reverse current rather than the feedback diode. *Figure 5* shows the base current and input signals during an on-off cycle. DC-DC converters, operating from the main propulsion battery, supply power for the base drive circuits.

The 525A peak current is based on a 315A RMS requirement in the PWM operating region, including 50A for high frequency ripple current and a 5% safety factor. Software-controlled hysteresis current bandwidth limits the transistor switching frequency to less than 5kHz. The polarized snubber limits the peak collector-emitter voltage to less than 360V for all conditions of supply voltage and load current.

Among the other inverter components are both electrolytic and high frequency capacitors connected to the DC bus. There is also a charging and discharging resistor and relay for initial start-up and final shut-down and current sensors to monitor AC output current.

Each power module was tested in a half-bridge circuit. The load inductance and resistance were selected to be equivalent to an actual inverter operating point. Load current was measured and used to control pulse width of the transistors in a closed-loop hysteresis current controller. This test simulated the actual worst-case operating conditions of the phase-leg inverter module.

The above tests used a 60Hz current reference and 4000Hz PWM chopping frequency. Peak load was 540A with a 50A peak-to-peak ripple. To ensure operation below the transistor's safe operating limit curve, maximum peak collector-emitter voltage was monitored during these tests. The peak is 280V (*Figure 6*), giving an overshoot ratio of 37% over the supply voltage.

The drive controller has two operating modes: constant torque and constant power[1]. In the constant torque region, the inverter is current-controlled using vector (field-oriented) PWM techniques. In the constant power region, control is based on torque angle orientation of the applied square wave (square wave mode). In the PWM mode, the machine phase currents and rotor angle are sampled and used to estimate and regulate the IPM motor torque and flux. Both the PWM and square wave modes were developed with the aid of computer simulation[2] and tested extensively in all four quadrants under steady state and transient conditions.

Inner current loops provide independent regulation of both the torque and flux-producing current vectors. Flux is programmed as a function of torque level to optimize drive system efficiency. The torque current command vector is generated from the torque error with conventional proportional plus integral compensation.

Three independent hysteresis band current regulators provide instantaneous control of the sinusoidal three-phase currents. In the constant power region the controller detects saturation of the current regulators and reconfigures the control laws to weaken the machine flux to establish the desired torque. Key feedback variables and estimators remain the same as in the PWM mode. Also, the flux estimator output detects an over-flux condition, which causes a transition back to the PWM control schemes.

The system uses three computers: one 8097 microcontroller and two TMS32010

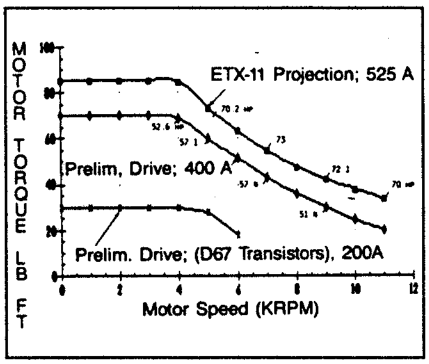

***Figure 2.** IPM Motor Torque vs Speed for 200A, 400A and ETX-II Inverters.*

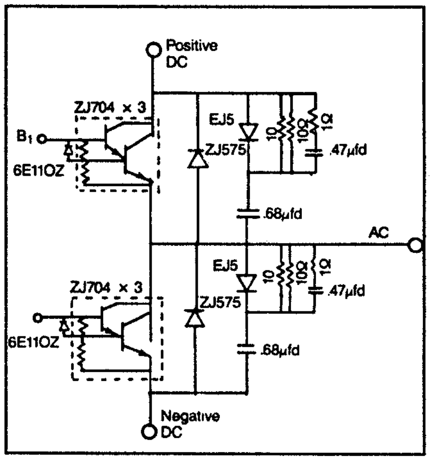

***Figure 4.** Phase-Leg Power Module.*

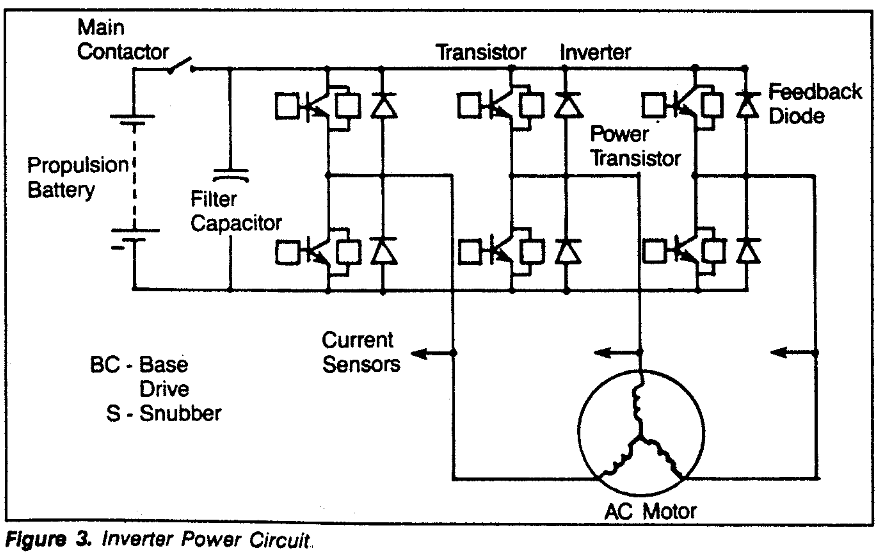

***Figure 3.** Inverter Power Circuit.*

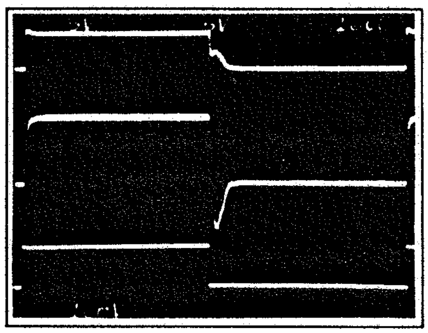

***Figure 5.** Base Current for Entire On-Off Cycle (10μsec/div).*
Top: Vout 5V/div.
Center: Iout 5A/div.
Bottom: Input 5V/div.

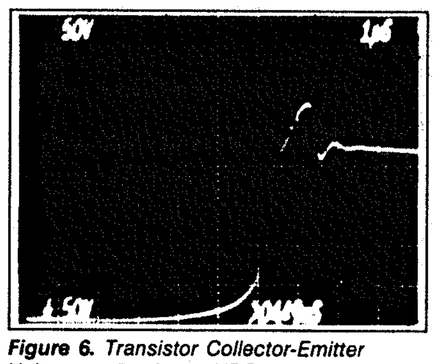

***Figure 6.** Transistor Collector-Emitter Voltage at 540A, 203VDC (1μsec/div).*

digital signal processors. The 5 MIPS signal processors provide the feedback and feedforward vector rotations and current vector regulation. The 8097 provides motor torque and flux estimation and regulation; it also performs drive system sequencing and supervisory tasks.

Packaging

Figure 7 shows the power module package with and without its cover. A 4×7 in. copper base plate holds the phase-leg power components and BeO isolates all the semiconductor chips from the base plate. Power connections (plus, minus and AC) are on the top surface for easy mounting to the low inductance DC supply. Connectors at each end of the module supply the base drive signals; these mate with connectors on the base drive printed circuit board. Three of these one-in.-high modules form the entire complement of power semiconductors for the inverter. *Figures 8* and *9* show the rest of the inverter packaging, including the baseplate, heat sink, temperature sensor, and overtemperature thermostat.

The power module employs a liquid-cooled system with air external pump and heat exchanger. Liquid cooling was selected because it minimizes size and weight. Previous studies of automotive inverters[3,4,5] indicated that a forced-air-cooled inverter would be larger and heavier than a liquid-cooled system using an external heat exchanger and pump. In addition, the major loss components (semiconductors and snubbers) provided a concentrated heat source with about 12 in.^{2} of cooling area available underneath the six transistors and two diodes. Plus, it was felt that it was doubtful that the large fin area required for forced-air cooling could be kept clean and efficient in an automotive environment.

Thermal Characteristics

Based on the projected 800W power dissipation in a module, the temperature rise from the junction to the bottom of the base plate was calculated to 10°C. The temperature rise was 33°C from the coolant exit to the base plate, measured with a flow of 2 gal/min. Therefore, the total thermal resistance is 0.054°C/W from junction to coolant exit. *Figure 8* shows the oval-shaped coolant channels and the enclosed interconnecting channels for the three modules. The coolant pump provides a constant circulating mixture of 50% water and glycol. The heat exchanger fan, thermostatically controlled by the coolant temperature, cycles on only when needed. Coolant temperature sensors provide feedback to the system controls that issue warnings to the operator, power limits to the inverter, or shut-down signals to the drive. To reduce pump power at very low temperatures, flow rate reduces to 1 gal/min.

The inverter enclosure with liquid cooling and a low inductance DC power bus measures 23.875″ (L) by 9.875″ (H) by 12.25″ (D), not including vehicle mounting brackets. The enclosure holds four subassemblies: power module/heat sink, conduction plate/storage capacitors, base drive and DC link voltage sensor.

The power module employs a liquid-cooled system with an external pump and heat exchanger.

The liquid coolant directly impinges the bottom of the power module base plate. Reservoirs measuring 0.06″ deep under each power module are connected in series via 0.5″ diameter coolant paths built into the heat sink. *Figure 8* shows the aluminum heat sink/top plate with these coolant paths exposed.

The heat sink subassembly contains the power transistor modules with internal snubbers and the aluminum top plate/heat sink with internal coolant piping. The precharge and discharge resistors are also attached to the top plate/heat sink, along with the coolant temperature sensor and overtemperature thermostats located on the coolant output port.

Each subassembly is populated and tested prior to inverter assembly. Only the enclosure frame, bottom cover plate, end plates and associated power components, which are not part of the major subassemblies, were directly assembled on the inverter enclosure frame.

Most of the components are accessible for replacement or monitoring by removing the inverter's side plates. *Figure 10* shows the fully-assembled inverter with its side plate removed. This arrangement provides easy access to each base drive card and the DC link voltage sense PC board. The only components that require inverter removal for parts replacement are the power modules and the storage capacitors.

Test Results

Inverter tests were performed on the prototype drive system consisting of a lead-acid battery pack, inverter/motor controls, inverter and IPM motor mounted in the test transaxle coupled to a dynamometer. A

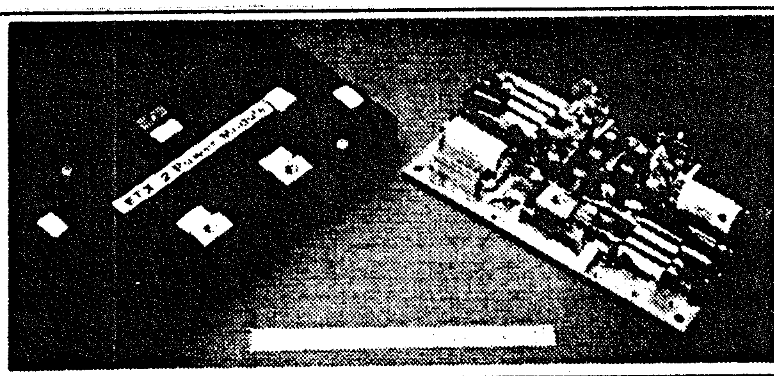

Figure 7. *Phase-Leg Power Module Package.*

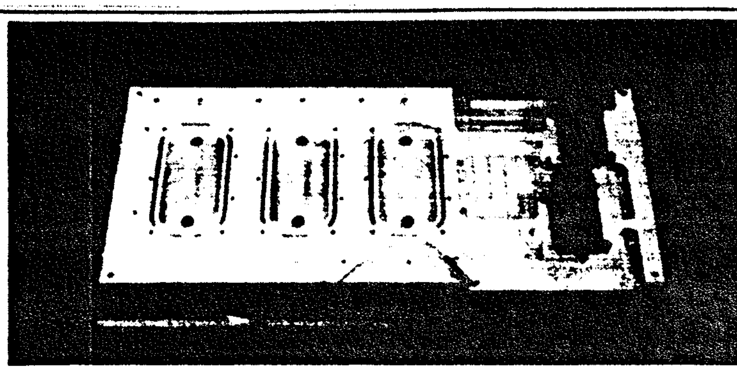

Figure 8. *Aluminum Heat Sink/Top Plate.*

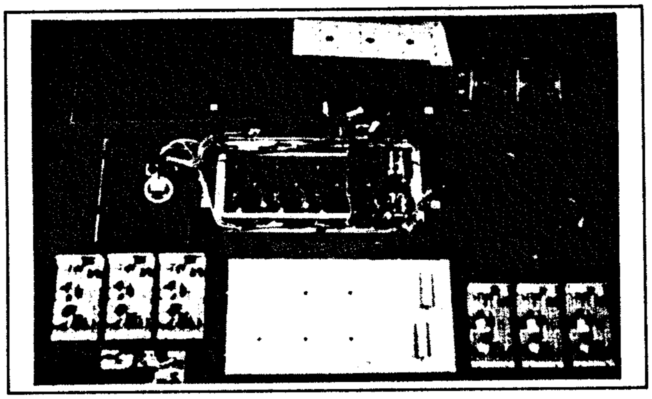

Figure 9. Inverter Enclosure and Components.

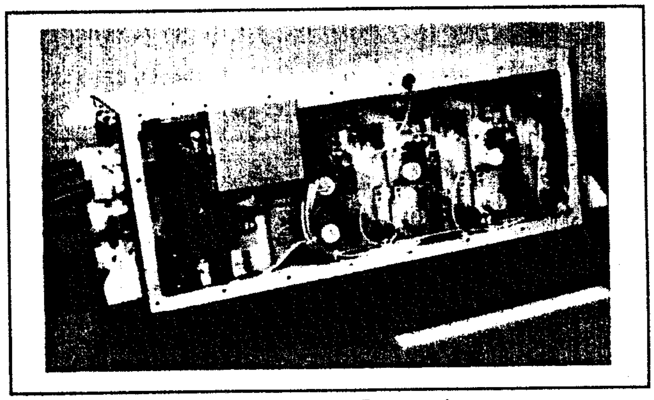

Figure 10. Inverter With Side Cover Removed.

computer-controlled data acquisition system[6,7] measured each drive system component input and output power. Vigorous system tests included: constant speed, maximum torque envelope step response with inertia loads; and first-to-second gear shifts with motor deceleration rates of 10,000 RPM/sec.

Figure 11 shows measured inverter efficiency vs motor speed and torque; the efficiency is 95-96.3% for 5,000 RPM and above and 40 lb-ft and above of torque. Inverter losses at a constant speed include: transistor/diode conduction and switching, base drive, and the DC link filter capacitor. Inverter efficiency increases with speed as shown in *Figure 12* for the maximum torque envelope.

Inverter efficiency vs DC link voltage for 9,000 RPM and 20 lb-ft torque is shown in *Figure 13*. One reason for reduced inverter efficiency at low DC link voltage and high speed, constant torque is that the output current must increase to supply the same output power as the DC link voltage decreases. Another reason is that the leading power factor decreases as the inverter supplies increased reactive power to reduce the motor back EMF.

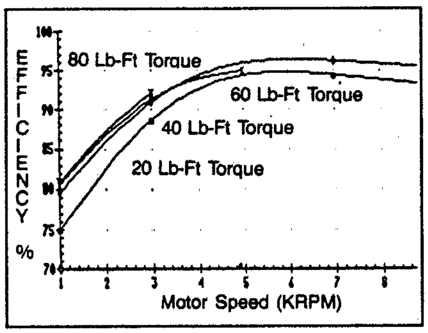

Figure 11. Inverter Efficiency vs Motor Speed (Prototype Drive, 135VDC Link).

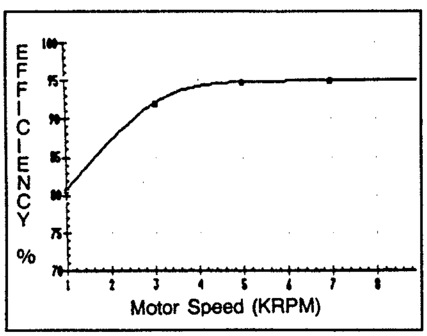

Figure 12. Inverter Efficiency for Maximum Torque Envelope (Prototype Drive, 135VDC Link).

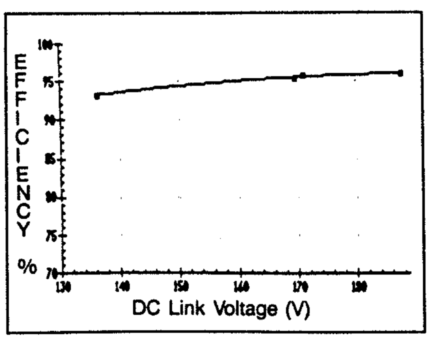

Figure 13. Inverter Efficiency vs DC Link Voltage (Prototype Drive, 9,000 RPM, 20 lb-ft Torque).

Acknowledgement

The work reported here was performed under contract number DE-AC07-85NV10418, funded by the U.S. Department of Energy and cost-shared by Ford Motor Company, the General Electric Company, and Powerplex Technologies Inc.

References

1. Bose, B.K., "A High Performance Inverter-Fed Drive System of an Interior Permanent Magnet Synchronous Motor," Conference Record of the 1987 IEEE/IAS Annual Meeting, pp. 269-276.
2. Bose, B.K., Szczesny, P.M., "Microcomputer-Based Control and Simulation of a Drive System Using an Interior Permanent Magnet Synchronous Machine," IEEE-IECON '87 Annual Meeting, Cambridge, MA. Nov. 2-6, 1987.
3. Oldenkamp, J.L., Peak, S.C., "Selection and Design of an Inverter Driven Induction Motor for a Traction Drive System," 1983 Annual Meeting IEEE Industrial Application Society, pp. 677-684.
4. ETX-I Powertrain Final Report, First-Generation Single-Shaft Electric Propulsion System Program, DOE/NV/10308-H1, Vol 1 of 2, U.S. Department of Energy, Contract No. DE-AC08-82NV10308, February 1987.
5. Patil, P.B., Stockton, T.R., and Peak, S.C., "Electric Transaxle System Design for an Advanced Electric Vehicle Powertrain," Paper No. 8324, EVC Expo, Dearborn, Michigan, 1983.
6. King, R.D., Koneda, P.T. "Advanced Electric Vehicle Powertrain (ETX-I) Performance - Component Testing," Eighth International Electric Vehicle Symposium," Washington, D.C., October 20-23, 1986.
7. Plunkett, A.B., Kliman, G.B., and Boyle, M.J., "Digital Techniques in the Evaluation of High-Efficiency Induction Motors for Inverter Drives," IEEE Transactions on Industry Applications, Vol. IA-21, No. 2, March/April 1985, pp. 456-463. □